MOLECULAR AND CELLULAR BIOLOGY, July 2003, p. 4586–4597 Vol. 23, No. 13
0270-7306/03/$08.00+0 DOI: 10.1128/MCB.23.13.4586–4597.2003

The Murine Nck SH2/SH3 Adaptors Are Important for the Development of Mesoderm-Derived Embryonic Structures and for Regulating the Cellular Actin Network

Friedhelm Bladt,[1,2] Elke Aippersbach,[1,2] Sigal Gelkop,[1,2] Geraldine A. Strasser,[3] Piers Nash,[1,2] Anna Tafuri,[4,5,6,7] Frank B. Gertler,[3] and Tony Pawson[1,2]*

Programme in Molecular Biology and Cancer, Samuel Lunenfeld Research Institute, Mount Sinai Hospital, Toronto, Ontario M5G 1X5,[1] Department of Molecular and Medical Genetics, University of Toronto, Toronto, Ontario M5S 1A8,[2] and Advanced Medical Discovery Institute,[4] Ontario Cancer Institute,[5] and Departments of Medical Biophysics[6] and Immunology,[7] University of Toronto, Toronto, Ontario M5G 2C1, Canada, and Department of Biology, Massachusetts Institute of Technology, Cambridge, Massachusetts[3]

Received 25 November 2002/Returned for modification 14 January 2003/Accepted 24 March 2003

Mammalian Nck1 and Nck2 are closely related adaptor proteins that possess three SH3 domains, followed by an SH2 domain, and are implicated in coupling phosphotyrosine signals to polypeptides that regulate the actin cytoskeleton. However, the in vivo functions of Nck1 and Nck2 have not been defined. We have mutated the murine Nck1 and Nck2 genes and incorporated β-galactosidase reporters into the mutant loci. In mouse embryos, the two Nck genes have broad and overlapping expression patterns. They are functionally redundant in the sense that mice deficient for either Nck1 or Nck2 are viable, whereas inactivation of both Nck1 and Nck2 results in profound defects in mesoderm-derived notochord and embryonic lethality at embryonic day 9.5. Fibroblast cell lines derived from Nck1$^{-/-}$ Nck2$^{-/-}$ embryos have defects in cell motility and in the organization of the lamellipodial actin network. These data suggest that the Nck SH2/SH3 adaptors have important functions in the development of mesodermal structures during embryogenesis, potentially linked to a role in cell movement and cytoskeletal organization.

Signaling by cell surface receptors commonly involves the recruitment of cytoplasmic targets into multiprotein complexes through specialized interaction domains. These domains provide a mechanism to couple different receptors to the core machinery that regulates cellular function and to provide a degree of specificity in signal transduction. Receptors with intrinsic or associated tyrosine kinase activity commonly recruit their targets through phosphotyrosine-containing motifs that bind the Src homology 2 (SH2) domains of cytoplasmic regulatory proteins (30, 45). Although some of these SH2-containing polypeptides have linked catalytic domains, others have an adaptor function and are comprised exclusively of interaction domains that nucleate the assembly of protein complexes around the activated receptor. Adaptors of the Nck, Grb2, and Crk families contain a single SH2 domain and various numbers of SH3 domains that typically bind to effector proteins through proline-rich peptide motifs. Each of these adaptors preferentially binds a distinct phosphotyrosine-containing motif through its SH2 domain and a specific group of signaling proteins through its SH3 domains. Grb2, for example, links phosphorylated Tyr-X-Asn sequences on activated receptor tyrosine kinases (RTKs) to proteins such as Sos and Gab1, involved in Ras/mitogen-activated protein (MAP) kinase and phosphatidylinositol 3′-kinase signaling (34, 36, 48).

* Corresponding author. Mailing address: Programme in Molecular Biology and Cancer, Samuel Lunenfeld Research Institute, Mount Sinai Hospital, 600 University Ave., Toronto, Ontario M5G 1X5, Canada. Phone: (416) 586-8262. Fax: (416) 586-8869. E-mail: pawson@mshri.on.ca.

Nck adaptor proteins possess three SH3 domains, followed by a C-terminal SH2 domain that binds optimally to pYDEP/D/V motifs (54). Both *Caenorhabditis elegans* (9) and *Drosophila melanogaster* (20) have a single Nck gene, whereas mammals have two Nck family members (Nck1/α and Nck2/β, also termed Grb4) (6, 9, 33, 38, 43, 62). The two murine Nck gene products exhibit 68% amino acid identity to one another, with most of the sequence variation being located in the linker regions between the SH3 and SH2 domains, and are 96% identical to their human counterparts (7). The Nck1 SH2 domain can bind a number of RTKs, such as those for platelet-derived growth factor (10, 41), epidermal growth factor (EGF) (35, 44), and ephrins (55), as well as tyrosine phosphorylated docking proteins, including p62^{Dok-1} (24) and p130^{Cas} (52). A variety of data have suggested that Nck proteins function to couple such phosphotyrosine signals to regulation of the actin cytoskeleton. Notably, the Nck1 SH3 domains bind selectively to proteins that control cytoskeletal organization, including N-WASP (46), WASP-interacting protein (1), and the WAVE1 complex (14). WASP and WAVE interact through their C termini with the Arp2/3 complex in a fashion that promotes actin branching and polymerization (for a review, see reference 57); this association with Arp2/3 is in turn regulated by a number of activators, including the Rac/Cdc42 GTPases, phosphoinositides, and Nck (16). Nck can bind directly through each of its SH3 domains to N-WASP, and these act cooperatively to stimulate N-WASP-Arp2/3-mediated actin polymerization in vitro (47). In contrast, Nck regulates WAVE1 indirectly by binding through its first SH3 domain to components of a transinhibitory complex (including NAP125

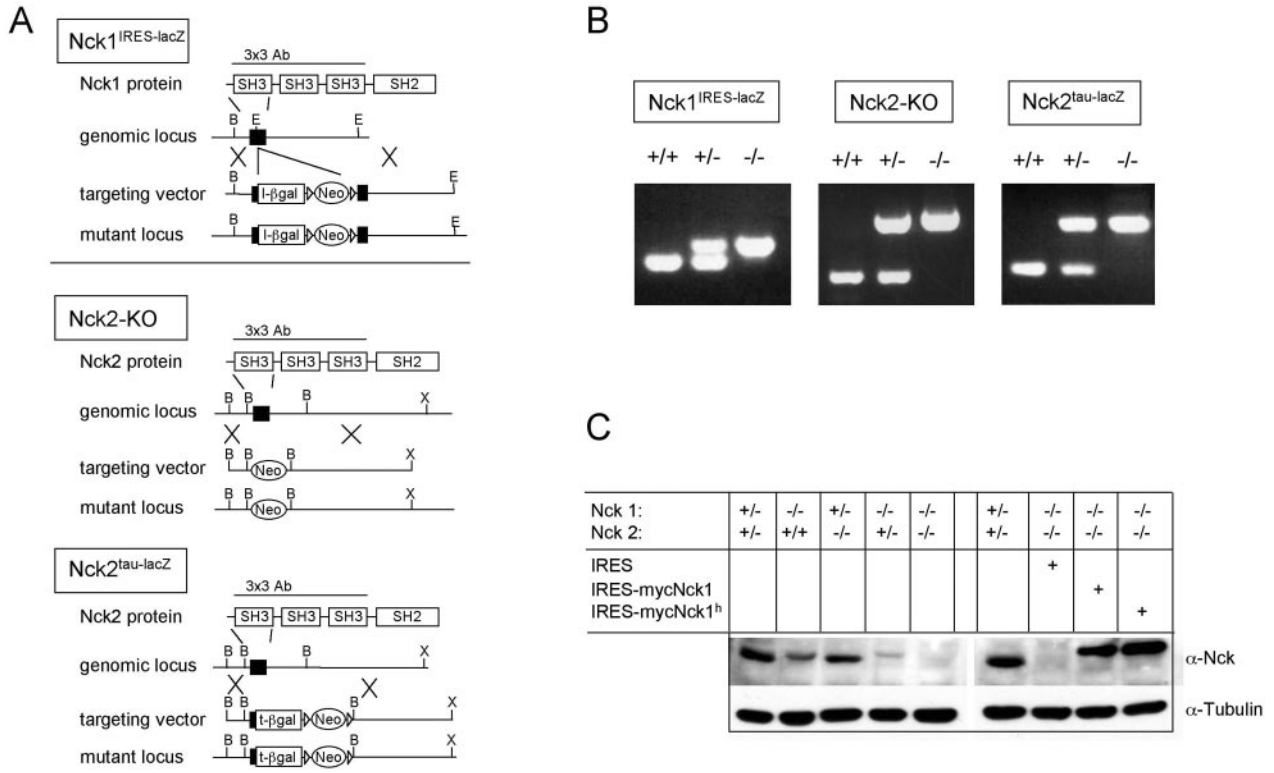

FIG. 1. Generation of Nck1- and Nck2-deficient mouse strains. (A) Schematic representation of the gene-targeting strategies used to mutate the Nck genes. The restriction maps of the Nck1 and Nck2 loci are indicated (B, *Bam*HI; E, *Eco*RI; X, *Xba*I). The Nck1$^{IRES\text{-}lacZ}$ targeting vector included an IRES-lacZ reporter gene cassette. The Nck2$^{tau\text{-}lacZ}$ targeting vector comprised a *tau-lacZ* reporter gene fused in frame with the first coding exon. The protein region employed to raise the 3x3 polyclonal antibody used for Western blot analysis is indicated. (B) Genotypic analysis of the mutant mouse strains by PCR. Primer combinations are indicated in the Methods. The WT and mutant bands were, respectively, of 210 and 280 bp for Nck1, 250 and 610 bp for Nck2^{ko}, and 170 and 280 bp for Nck2$^{tau\text{-}lacZ}$ mutant mouse strains. (C) Expression of the Nck genes was assessed by Western blotting of protein extracts of MEFs with the indicated genotypes. Western blots of protein extracts of mutant MEFs infected with IRES-EGFP and myc-tagged Nck1-IRES-EGFP retroviral vectors are also shown.

and PIR121) that is released from WAVE1 upon association with Nck or Rac1, leading to enhanced actin polymerization (14).

Nck1 also interacts through its SH3 domains with Ste20-like protein-serine/threonine kinases. For example, the second Nck1 SH3 domain binds to the Pak1 serine/threonine kinase (19) and regulates membrane localization and kinase activity in conjunction with Cdc42. Once activated Pak1 phosphorylates substrates such as LIM kinase, which in turn phosphorylates and inhibits cofilin, and MLCK, involved in actin/myosin organization (15, 50). Pak1 also has a scaffolding function, through its ability to bind the SH3 domain of PIX, a guanine nucleotide exchange factor for the Cdc42 and Rac1 GTPases that can induce membrane ruffling, and is enriched in Cdc42 and Rac1-driven focal complexes (42). The second Nck1 SH3 domain can also recruit the Nck-interacting serine/threonine kinase, which is implicated in coupling RTKs such as Eph receptors to integrins and the JNK stress-activated MAP kinase (2, 56).

Less is known concerning the binding properties and biological function of Nck2, although these are in general rather similar to Nck1 (6). Nck2 has been identified as selectively interacting through its third SH3 domain with the LIM4 domain of PINCH, a protein involved in integrin signaling (62). In addition, the Nck2 SH2 domain specifically binds to tyrosine phosphorylated B-type ephrins and links B-ephrin reverse signaling to cytoskeletal regulatory proteins (11). Nck2 has also been proposed to have a unique role in linking the β platelet-derived growth factor-receptor to actin polymerization in mouse NIH 3T3 fibroblast (10).

Genetic data from *Drosophila* indicate that the *Drosophila* Nck orthologue, Dreadlocks (Dock), signals through PAK to mediate the proper guidance and targeting of photoreceptor (R) growth cones, a finding consistent with the view that Nck proteins may have a physiologically important impact on the cytoskeleton (20, 23). Furthermore, the interaction of Dock with the *Drosophila* Nck-interacting serine/threonine kinase orthologue Misshapen may also contribute to R axon targeting (49, 56). The function of Nck proteins in vertebrates has been addressed by the use of dominant inhibitory SH domain mutants, which have implicated Nck in dorsoventral axis development during embryogenesis in *Xenopus* (61).

In addition to their role in normal cellular function, Nck adaptors are involved in the cellular response to viral and bacterial pathogens. The A36R gene product of vaccinia virus binds the Nck SH2 domain through a tyrosine phosphorylated motif; Nck, in turn, recruits WASP-interacting protein and the actin regulator N-WASP, stimulating the actin-based motility

of the viral particle (17). In a related fashion, we have found that the Tir protein of enteropathogenic *Escherichia coli* becomes tyrosine phosphorylated at the plasma membrane of infected cells at a site that binds Nck, and thus N-WASP and Arp2/3, correlating with a massive actin polymerization at the site of bacterial attachment (22). In the absence of Nck proteins (see below), enteropathogenic *E. coli* fails to induce cytoskeletal reorganization in the host cell.

Despite these advances, there are no genetic data that directly address the physiological functions of vertebrate Nck gene products in vivo or their role in controlling the actin cytoskeleton in normal cultured cells. To address these issues, we generated mouse strains lacking Nck1, Nck2, or both Nck genes. Our findings indicate that the two Nck proteins have overlapping and mutually compensatory functions. However, inactivation of both Nck genes results in early embryonic lethality and profound defects in mesoderm-derived embryonic structures. Using fibroblast cell lines derived from Nck1$^{-/-}$ Nck2$^{-/-}$ embryos, we provide genetic evidence for a role of the Nck proteins in normal cell motility and lamellipodium formation, which may pertain to their function in embryogenesis.

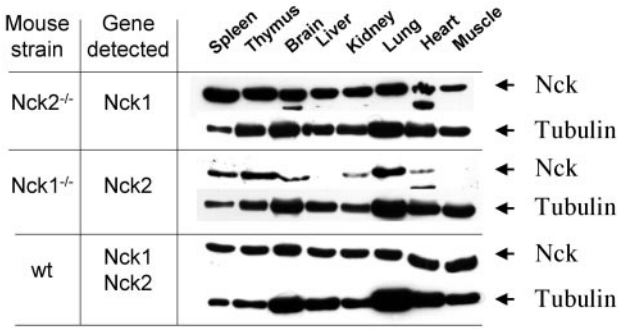

FIG. 2. Differential pattern of expression of Nck1 and Nck2 in adult tissues. The expression of Nck1 and Nck2 was assessed in various tissue extracts from Nck1$^{-/-}$ Nck2$^{-/-}$ mutants and WT mice. Equivalent amounts of tissue extracts (determined by Bio-Rad assay) were probed with the 3x3 polyclonal antibody, recognizing the first SH3 domain of Nck1 and Nck2. Since this region was deleted in our targeting strategies, we used tissues from Nck2$^{-/-}$ and Nck1$^{-/-}$ mutants to assess the expression of Nck1 and Nck2, respectively. Membranes were stripped and reblotted with anti-β-tubulin antibody. Arrowheads mark the position of the indicated protein bands. The results are representative of two independent experiments.

MATERIALS AND METHODS

Generation of Nck1$^{-/-}$ Nck2$^{-/-}$ mutant mice. For construction of the different targeting vectors, genomic fragments were isolated from a 129/SV-Ola library. The Nck1$^{IRES\text{-}lacZ}$ vector contained a 5.4-kb genomic fragment including the first coding exon. The internal ribosome entry site (IRES)-lacZ-loxP-pgk-Neo-loxP cassette was introduced into an *Eco*RV restriction site in the first coding exon, 23 codons downstream of the start codon, separating the genomic fragment into a 1.8-kb 5′ arm and a 3.6-kb 3′ arm. The Nck2^{ko} vector contained a 2.5-kb *Bgl*II/*Bgl*II fragment as a 5′ arm and a 4.2-kb *Bgl*II/*Xba*I fragment as a 3′ arm. A pgk-Neo cassette was inserted between the two arms, replacing a 2.8-kb genomic fragment, including the first coding exon of the Nck2 gene. The Nck2$^{tau\text{-}lacZ}$ targeting vector contained a tau-lacZ-loxP-Neo-CMV-loxP cassette fused to the N-terminal part of the first coding exon, resulting in a fusion protein consisting of the first 40 amino acids of Nck2 and the tau-lacZ gene. A 2.7-kb *Bgl*II-*Sac*I fragment and a 4.2-kb *Bgl*II/*Xba*I fragment were used as 3′ and 5′arms, respectively. Embryonic stem (ES) cells were electroporated with the linearized targeting vectors and selected with G418. Positive ES clones identified by Southern blotting were injected into ICR blastocysts to generate heterozygous mutant mice.

PCR screening of gene-targeted mouse strains. Template DNA for genomic PCR was isolated from ear tissue as described previously (25). For each mutant mouse line, four primers were used to screen for wild-type (WT), heterozygous, and homozygous mutant mice. For the Nck1 locus, primers were designed up- and downstream of the insertion point (*Eco*RI restriction site) of the Neo cassette and the β-galactosidase region; for the Nck2^{ko} locus, primers were designed within the deleted WT locus and the neomycin gene; for the Nck2$^{tau\text{-}lacZ}$ locus, primers were designed within the deleted WT locus and the β-galactosidase region, respectively. To genotype Nck1$^{IRES\text{-}lacZ}$, the following primers were used: 5′-GCATGTAGACAATTACACTTCAGCACC-3′, 5′-ATTCATGGAATTTCGAACTCGCCACC-3′, 5′-CTGATTGAAGCAGAAGCCTGCGATG-3′, and 5′-TATTGGCTTCATCCACCACATACAGG-3′. To genotype NCK2^{KO}, the following primers were used: 5′-CTACACTGCCCAGCAGGACCAGG-3′, 5′-CACATACAGATACACACACGCTGAAG-3′, 5′-CCAATGGCAAAGGTGATCATGACGG-3′ and 5′-CGCCTTCTATCGCCTTCTTGACGAG-3′. To genotype Nck2$^{tau\text{-}lacZ}$, the following primers were used: 5′-GAGGAATGCTGCCAACAGGACAGG-3′, 5′-CACATACAGATACACACACGCTGAAG-3′, 5′-CTGATTGAAGCAGAAGCCTGCGATG-3′, and 5′-TATTGGCTTCATCCACCACATACAGG-3′.

Western blotting. Embryonic day 8.5 (E8.5) embryos were homogenized in phospholipase C lysis buffer by using a Teflon homogenizer as described previously (31).

β-Galactosidase staining of whole embryos and tissue sections. Embryos and tissue sections were fixed in 1.6% formaldehyde–0.2% glutaraldehyde, washed in *lacZ* wash buffer (2 mM $MgCl_2$, 0.02% NP-40, 0.01% deoxycholate, 0.1 M sodium phosphate buffer [pH 7.3]) and stained with X-Gal [5-bromo-4-chloro-3-indolyl-β-D-galactopyranoside; 1 mg/ml in wash buffer containing 2.12 mg of $K_4Fe(CN)_6$, 1.64 mg of $K_3Fe(CN)_6$ or 0.5 mg of nitroblue tetrazolium (NBT)/ml at 37°C]. Whole-mount in situ hybridization on Nck1 and/or Nck2 mutant embryos was performed as previously described (51).

Antibodies. Antibody recognizing murine Nck1 and Nck2 was obtained from rabbits immunized with a glutathione *S*-transferase fusion protein, containing the three SH3 domains of human NCK1 (residues 1 to 255). Anti-β-tubulin mouse specific monoclonal antibody was purchased from Sigma.

Establishment of MEFs, cell culture, and wounding assays. To establish mouse embryonic fibroblast (MEF) lines from WT and Nck mutant embryos, E8.5 embryos were dispersed in cell dissociation buffer (Sigma). The resulting MEFs were cultured in Dulbecco modified Eagle medium plus 10% fetal bovine serum until they underwent crisis. Wounding assays were performed as previously described (29).

Ultrastructural analysis of MEFs. Platinum replica electron microscopy and ATP depletion-recovery assay were performed as previously described (59).

RESULTS

Targeted disruption of the Nck1 and Nck2 genomic loci. The gene encoding murine Nck1 was inactivated by inserting an IRES–β-galactosidase cassette into the first coding exon, 29 nucleotides downstream of the start codon (Nck1$^{IRES\text{-}lacZ}$, Fig. 1A). An Nck1$^{IRES\text{-}lacZ}$ heterozygous ES cell line that had undergone homologous recombination was used to generate chimeric mice, which were crossed to ICR females to obtain Nck1$^{IRES\text{-}lacZ}$ heterozygous mice. Intercrossing of Nck1 heterozygous animals yielded Nck1$^{-/-}$ mice at approximately Mendelian frequencies, as assessed by PCR (Fig. 1B) and Southern blot analysis (data not shown). To disrupt the Nck2 gene, two independent targeting constructs were designed (see Fig. 1A). In the Nck2^{ko} targeting vector, the first coding exon was replaced by a pgk-Neo cassette. In the Nck2$^{tau\text{-}lacZ}$ targeting vector, a tau–β-galactosidase cassette replaced the C-terminal part of the first coding exon (encoding amino acids 22 to 76) and part of the intron sequences. The Nck2^{ko} and Nck2$^{tau\text{-}lacZ}$ targeting vectors were independently electroporated into ES cells and a correctly targeted ES cell clone for each vector was used to obtain chimeras. In both cases, inter-

TABLE 1. In vivo inactivation of Nck1 and Nck2 results in embryonic lethality at E9.5[a]

Dissection time point (day)	No. of surviving embryos or mice from $Nck1^{-/-}$ $Nck2^{+/-}$ × $Nck1^{+/-}$ $Nck2^{-/-}$ intercrosses			
	$Nck1^{+/-}$ $Nck2^{+/-}$	$Nck1^{-/-}$ $Nck2^{+/-}$	$Nck1^{+/-}$ $Nck2^{-/-}$	$Nck1^{-/-}$ $Nck2^{-/-}$
P21	61	57	51	0
E12	12	14	11	0
E10	25	22	27	7
E8	30	31	26	29

[a] Loss of in vivo function of either Nck1 or Nck2 does not result in any gross morphologic or functional abnormalities. In contrast, mutation of both Nck1 and Nck2 genes is incompatible with a normal embryonic development and results in death in utero at around gestational day 9.5. P, postnatal day.

crossing of heterozygous $Nck2^{ko}$ and $Nck2^{tau\text{-}lacZ}$ mice yielded homozygous mutants at approximately Mendelian frequencies. Mice that were homozygous mutant for either Nck1 or Nck2 proved to be healthy and fertile, and lacked any gross morphological or functional abnormalities.

To determine the effects of the $Nck1^{IRES\text{-}lacZ}$ and $Nck2^{ko}$ mutations on expression of the Nck proteins, we performed Western blot analysis on extracts from E9.5 mutant embryos (data not shown), on adult tissues from mice lacking either Nck1 or Nck2 (Fig. 2), and on $Nck1^{-/-}$ $Nck2^{-/-}$ embryonic fibroblast cell lines (Fig. 1C). Using a polyclonal antibody (3x3) raised to the three SH3 domains that recognizes both Nck1 and Nck2, the full-length 47-kDa Nck1/Nck2 proteins were readily identified in WT and heterozygous embryos and fibroblasts but were not detectable in similar samples derived from cells or tissues homozygous for both Nck genes (i.e., $Nck1^{IRES\text{-}lacZ-/-}$ $Nck2^{ko-/-}$ mutants) (Fig. 1C). Epitope mapping with Nck2 peptides revealed that the 3x3 antibody primarily recognizes a conserved motif in the first SH3 domain (residues 51 to 56), which is encoded by the first exon deleted by the $Nck1^{IRES\text{-}lacZ}$ and $Nck2^{ko}$ mutations (data not shown). We therefore cannot exclude the possibility that the mutant loci may still encode truncated polypeptides. However, a second antibody raised against the Nck1 linker region between the third SH3 domain and the SH2 domain did not identify any smaller C-terminal polypeptides that might arise from the retained Nck1 sequences (data not shown). A conclusive analysis has not yet been possible with similar Nck2-specific antibodies. The available Western analysis data, coupled with the phenotype of the doubly mutant mice (see below), suggest that we have functionally inactivated both genes. Furthermore, the lack of phenotypic abnormalities in single mutant mice would argue against the possibility that we have generated dominant-negative alleles.

Taken together, our findings indicate that in vivo inactivation of either member of the Nck family does not result in gross morphological or functional alterations in mice and suggest

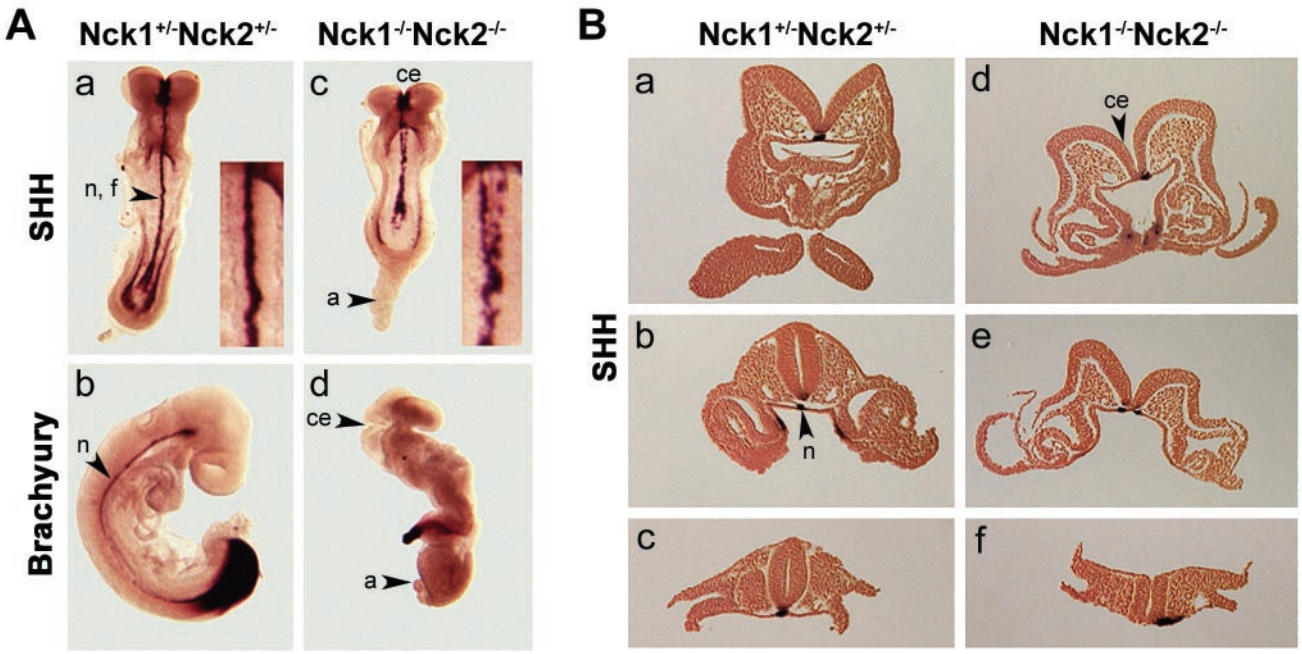

FIG. 3. Concomitant loss of Nck1 and Nck2 functions results in multiple morphological abnormalities and lack of axial rotation. (A) Shh and Brachyury staining of $Nck1^{+/-}$ $Nck2^{+/-}$ and $Nck1^{-/-}$ $Nck2^{-/-}$ embryos at E8.5 (a and c) and E9.5 (b and d). In $Nck1^{+/-}$ $Nck2^{+/-}$ embryos, Shh stained the notochord, floor plate, and endodermal cells of the hind- and foregut (a). In $Nck1^{-/-}$ $Nck2^{-/-}$ embryos, Shh staining could be detected in the notochord floorplate and endodermal cells. The notochord floorplate was bifurcated and disrupted along the posterior-anterior axis (c). Brachyury expression is evident in the tail bud and notochord of E9.5 control embryo (b). $Nck1^{-/-}$ $Nck2^{-/-}$ embryos (d) did not "turn," and the allantois did not fuse with the chorion and acquired a balloon-like structure. The headfolds were not closed. Fragmentary brachyury staining was visible in the tail bud and along the posterior-anterior axis. (B) Sections from $Nck1^{+/-}$ $Nck2^{+/-}$ and $Nck1^{-/-}$ $Nck2^{-/-}$ mutant E8.5 embryos stained with Shh. In $Nck1^{+/-}$ $Nck2^{+/-}$ embryos, notochord (a to c), floor plate (a to c), and endodermal precursor cells (b) were positive for Shh. In mutant embryos, Shh staining revealed displacement beside the midline (d and f) and bifurcation (e) of notochord and floor plate. Abbreviations: n, notochord; f, floorplate; a, allantois; ce, cephalic folds.

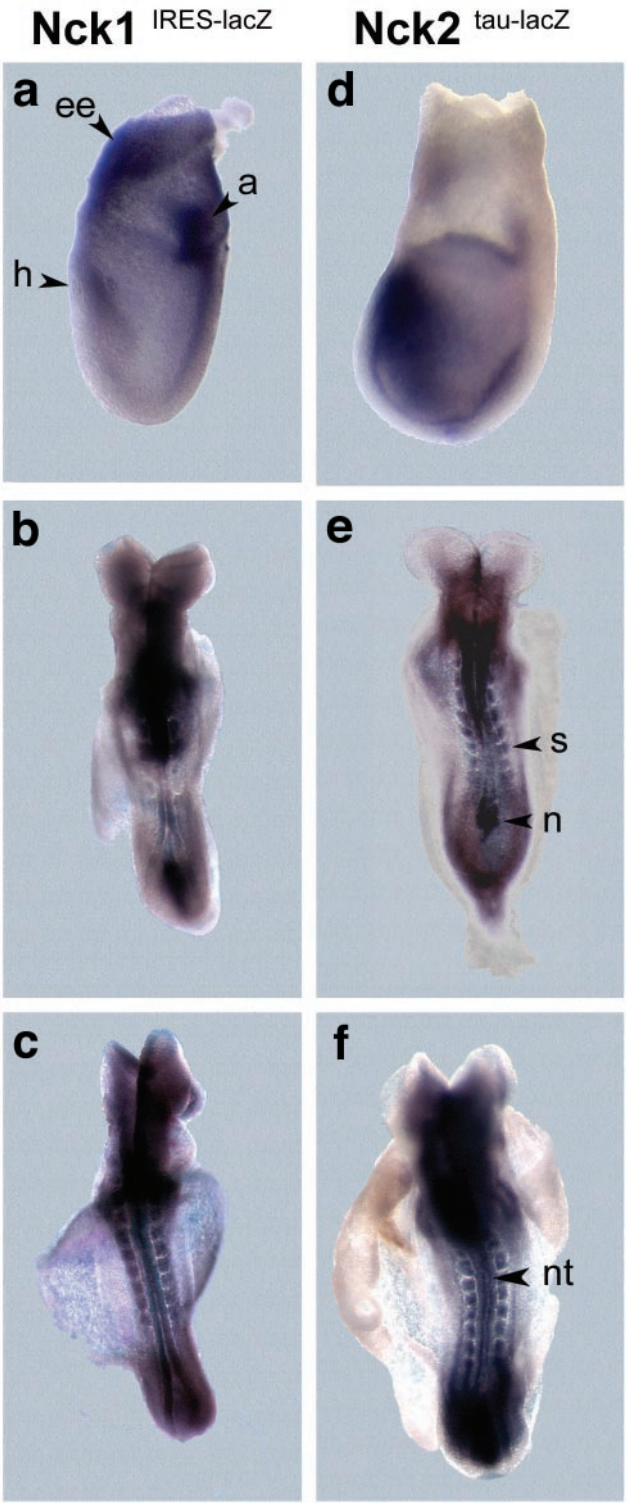

FIG. 4. Expression pattern of Nck1 and Nck2 at E7.5 and E8.5. β-Galactosidase activity was exhibited by E7.5 (a and d) and E8.5 (b, c, e, and f) embryos heterozygous for the $Nck1^{IRES\text{-}lacZ}$ and $Nck2^{tau\text{-}lacZ}$ loci. Although weak β-galactosidase activity was detected throughout both Nck1 and Nck2 heterozygous embryos, strong expression of both the Nck1 and Nck2 genes localized to the allantois (a), headfold (h), and extraembryonic (ee) tissues (panels a and d). At E8.5 both genes were expressed in the node (n), somites (s), and neural tube (nt; panels b, c, e, and f). In $Nck1^{IRES\text{-}lacZ}$ embryos, weak staining was also found in the yolk sac.

either that Nck function is not essential for development or that Nck1 and Nck2 have redundant activities.

Expression of Nck1 and Nck2 in adult tissues. To investigate whether Nck1 or Nck2 might potentially have any unique functions, we explored their expression patterns in various adult tissues. A number of tissues isolated from 6- to 8-week-old $Nck1^{-/-}$ and $Nck2^{-/-}$ mutant mice were examined by Western blot analysis for expression of Nck1 or Nck2 proteins (Fig. 2). Nck1 and Nck2 were detected with the Nck1/Nck2 cross-reactive 3x3 antibody, which recognizes the first SH3 domain that is conserved between Nck1 and Nck2 and deleted in both $Nck1^{-/-}$ and $Nck2^{-/-}$ mutants. Although similar amounts of Nck1 protein were detected in all tissue extracts tested, Nck2 appeared to be expressed at higher levels in the thymus, spleen, and lungs; was expressed at lower levels in the heart, kidney, and brain; and was not detectable in the liver and skeletal muscle. These data indicate that Nck1 and Nck2 have distinct, albeit overlapping, patterns of expression in adult tissues, raising the possibility that they may have some unique biological activities.

Concomitant loss of Nck1 and Nck2 function results in early embryonic lethality. To pursue the in vivo functions of the Nck proteins, $Nck1^{IRES\text{-}lacZ}$ and $Nck2^{ko}$ mutants were crossed in an effort to obtain doubly mutant mice (referred to as $Nck1^{-/-}$ $Nck2^{-/-}$). Breeding of heterozygous Nck1/Nck2 mutant mice resulted in the generation of $Nck1^{+/-}$ $Nck2^{-/-}$ and $Nck1^{-/-}$ $Nck2^{+/-}$ mutant mice, as assessed by PCR and Southern blot analysis (data not shown), which proved to be healthy and fertile. However, intercrosses of $Nck1^{-/-}$ $Nck2^{+/-}$ with $Nck1^{+/-}$ $Nck2^{-/-}$ mice never yielded viable double homozygous offspring, suggesting that the mutation of both Nck1 and Nck2 genes resulted in embryonic lethality (Table 1). To identify the stage of development specifically affected by the loss of both Nck proteins, litters from $Nck1^{-/-}$ $Nck2^{+/-}$ × $Nck1^{+/-}$ $Nck2^{-/-}$ intercrosses were dissected at different gestational time points. As summarized in Table 1, whereas $Nck1^{-/-}$ $Nck2^{-/-}$ embryos were identified at approximate Mendelian frequencies at E8.5, their number was reduced to about one-third of the expected level at E10.5. By E12.5, no viable $Nck1^{-/-}$ $Nck2^{-/-}$ mice could be found, as judged by the presence or absence of a beating heart.

Defective chorion-allantoic fusion and axial rotation in $Nck1^{-/-}$ $Nck2^{-/-}$ embryos. To gain a better understanding of the abnormalities resulting from loss of Nck1 and Nck2, we carried out a detailed morphological and histological analysis of E8.5 and E9.5 embryos. $Nck1^{-/-}$ $Nck2^{-/-}$ embryos exhibited a significant developmental delay and smaller size compared to littermate controls (Fig. 3A). In particular, three main defects could be identified: lack of chorion allantoic fusion, deficient axial rotation, and impaired closure of the cephalic neural folds. In $Nck1^{-/-}$ $Nck2^{-/-}$ embryos the allantois was misshapen and developed into a balloon-like structure (Fig. 3Ad), growing anteriorly toward the headfold structures (data not shown). This defect resulted in a lack of a chorioallantoic placenta and a failure to establish definitive embryonic circulation. Axial rotation (or "turning"), a process beginning at E8.5 that leads to reversion of the orientation of the germ layers, did not take place in the absence of the Nck proteins, and $Nck1^{-/-}$ $Nck2^{-/-}$ embryos had still not turned at E9.5 (Fig. 3Ad). Furthermore, in E8.5 $Nck1^{-/-}$ $Nck2^{-/-}$ embryos

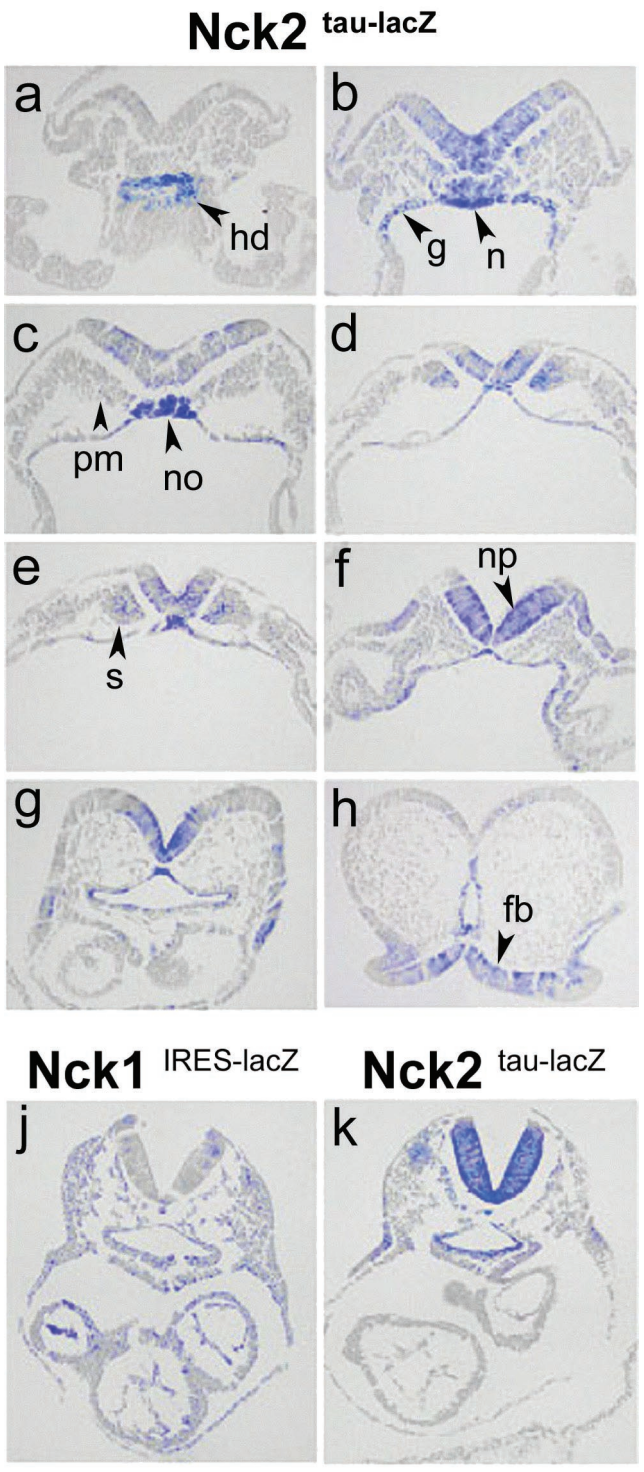

FIG. 5. Comparative analysis of the expression pattern of Nck1 and Nck2 at E8.5. Transverse sections of X-Gal-stained heterozygous $Nck2^{tau\text{-}lacZ}$ and $Nck1^{IRES\text{-}lacZ}$ E8.5 embryos. In heterozygous $Nck2^{tau\text{-}lacZ}$ embryos, β-galactosidase activity was detected in the caudal extremity of hindgut diverticulum (a); endodermal lining of hind-, mid-, and foregut (b to g); caudal region of notochord (b); notochordal plate (c); notochord (f and g); neural plate (b to f); neuroepithelium of prospective forebrain region (h); paraxial mesoderm (b and c); and somites (d and e). (j and k) Comparative analysis of similar transverse sections from homozygous $Nck1^{IRES\text{-}lacZ}$ and $Nck2^{tau\text{-}lacZ}$ mutants at E8.5 revealed expression of both genes in most tissues. However, whereas the neural tube was noticeably wavy, and at later stages the head appeared dilated as a result of a failure to close the cephalic neural folds. Morphological analysis revealed closure of the neural tube at the level of the otic vesicle, indicating that neurulation was properly initiated and had continued through the hindbrain but had not progressed beyond the midbrain-forebrain boundary (Fig. 3Ac and d).

To pursue the origin of these defects, the expression patterns of markers for axial mesoderm (Brachyury and Sonic hedgehog [Shh]) and paraxial mesoderm (mox-1) were assessed in E8.5 and E9.5 embryos by RNA in situ hybridization (8, 13, 64). The overall expression of Shh and Brachyury was comparable in $Nck1^{-/-}$ $Nck2^{-/-}$ embryos and control littermates. Shh was expressed in the notochord, neural floorplate, and gut regions (Fig. 3Aa and c), whereas Brachyury was expressed in the primitive streak and migrating notochordal precursors (data not shown). However, in E8.5 $Nck1^{-/-}$ $Nck2^{-/-}$ embryos, Brachyury (data not shown) and Shh (Fig. 3Ac) exhibited abnormal fragmentation and bifurcation at the level of the notochord. In E9.5 $Nck^{-/-}$ $Nck2^{-/-}$ embryos, Brachyury expression was only detectable in the deformed "tailbud" and a few cell clumps along the anterior-posterior axis (Fig. 3Ad).

In serial sections of E8.5 embryos that had undergone in situ hybridization for Shh RNA, the discontinuous pattern of Shh staining in the notochord appeared to be due not only to loss of Shh expression but also to anatomic malformations of the notochord (data not shown). Where detectable, Shh expression in the floorplate appeared bifurcated (Fig. 3Be) and/or located beside the midline of the notochord (Fig. 3Bd to f). Although the initial development (two to four somites) of the notochord was indistinguishable in $Nck1^{-/-}$ $Nck2^{-/-}$ embryos and control littermates (data not shown), the absence of the Nck proteins resulted in rapid notochord degeneration. Mox-1 staining confirmed the presence of somites but revealed different degrees of disorganization of the rostral somites of older $Nck1^{-/-}$ $Nck2^{-/-}$ embryos (9 to 13 somites [data not shown]). Taken together, our findings indicate that the Nck proteins in aggregate play a crucial role in mammalian embryogenesis and, in particular, are important for the proper development of mesoderm-derived structures.

Expression pattern of Nck1 and Nck2 during embryonic development. To better understand the specific roles of Nck1 and Nck2 in embryonic development, we compared their patterns of expression by assessing the temporal and spatial appearance of β-galactosidase activity in $Nck1^{IRES\text{-}lacZ}$ and $Nck2^{tau\text{-}lacZ}$ E7.5 to E10 embryos. At early and late headfold stages, both Nck1 and Nck2 were expressed in the head process, allantois, and extraembryonic tissue (Fig. 4a and d). Low but significant levels of expression of both Nck genes were found throughout the embryo. By midgastrulation (E8.5), Nck1 was expressed at low levels throughout the embryo (Fig. 4b and c and 5j), whereas Nck2 was highly expressed in meso-

Nck1 was expressed throughout the embryo, Nck2 exhibited a more restricted pattern of expression and was undetectable in the hearts of $Nck2^{tau\text{-}lacZ}$ embryos. Abbreviations: hd, hindgut diverticulum; g, hind-, mid-, and foregut; n, notochord; no, notochordal plate; np, neural plate; fb, forebrain; pm, paraxial mesoderm; s, somites.

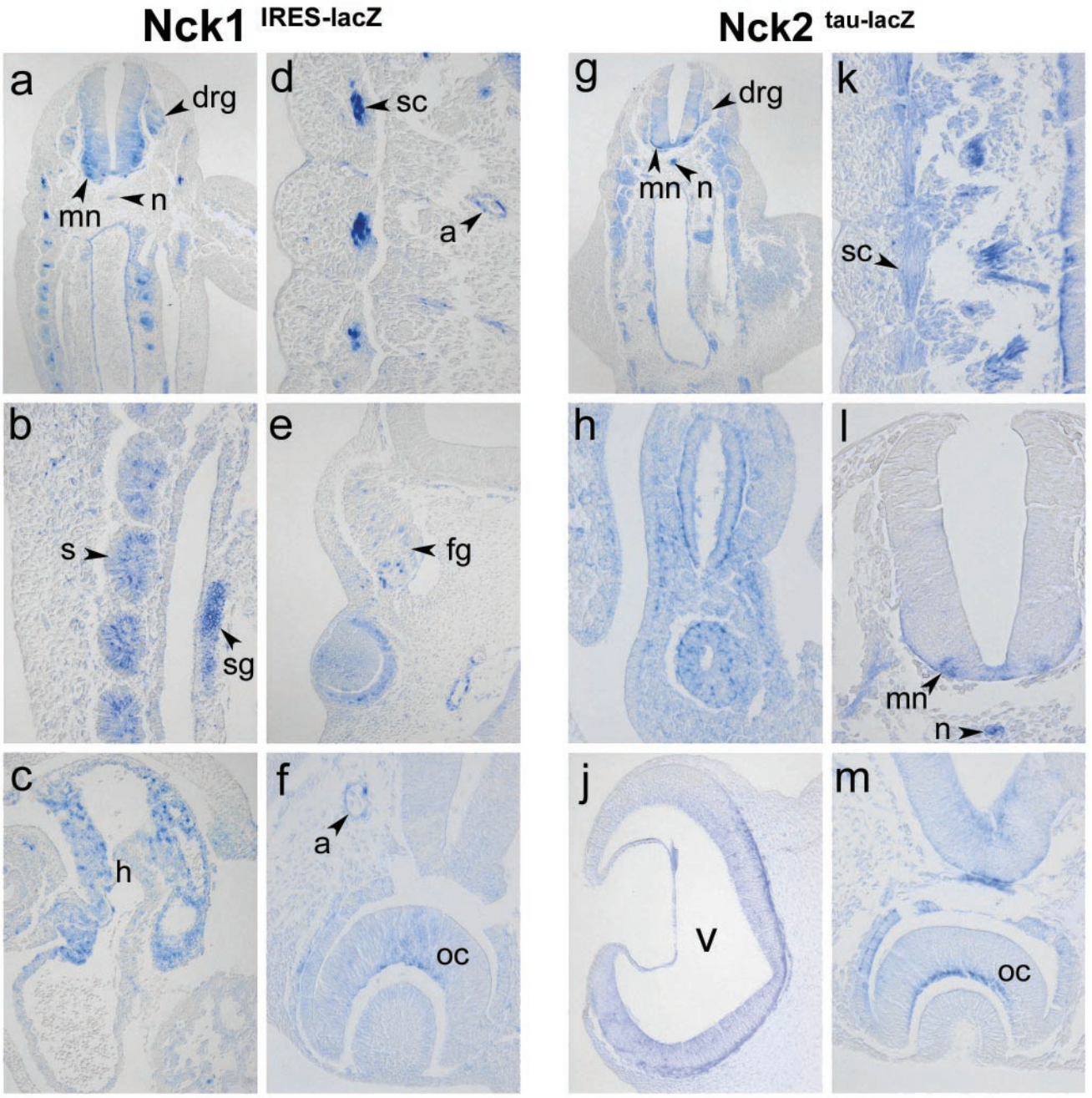

FIG. 6. Nck1 and Nck2 have highly overlapping expression patterns and are particularly prominent in the developing nervous system. Transverse sections of X-Gal-stained $Nck1^{IRES\text{-}lacZ}$ and $Nck2^{tau\text{-}lacZ}$ embryos at E10.5. Nck1 and Nck2 were highly expressed in neural structures such as motorneurons (a, g, k, and l), dorsal root ganglia (a and g), facial ganglia (e), sympathetic trunk ganglia (b), the inner layer of optic cup (f and m, future nervous layer of the retina), and the neuroepithelium of the ventricles (j). However, expression was also detected in nonneural structures such as the notochord (a, g, and l), somites (a, b, and g), sclerotome (a, d, and k), and arteries (d to f and m). Interestingly, the Nck proteins were differentially expressed in the arterial chamber of the heart (c), where the expression of Nck1, but not Nck2, could be detected. Abbreviations: m, motorneurons; drg, dorsal root ganglia; fg, facial ganglia; sg, sympathetic trunk ganglia; oc, optic cup; v, ventricle; n, notochord; s, somites; sc, sclerotome; a, arteries; h, heart.

derm- and endoderm-derived structures, such as the node, as well as in the neuroectoderm (Fig. 5). At E10.5, both Nck1 and Nck2 were strongly expressed in the ganglia, motorneurons, developing optic cup, ventricular neuroepithelium, gut, stomach, arteries, and somites, particularly in the sclerotome (Fig. 6). In addition, Nck1 was also expressed in the arterial chamber of the developing heart (Fig. 6c). Thus, the expression of Nck1 and Nck2 in the neural fold, notochord, rostral somites, allantois, and extraembryonic tissues matches both physically and chronologically the defects observed in $Nck1^{-/-}$ $Nck2^{-/-}$

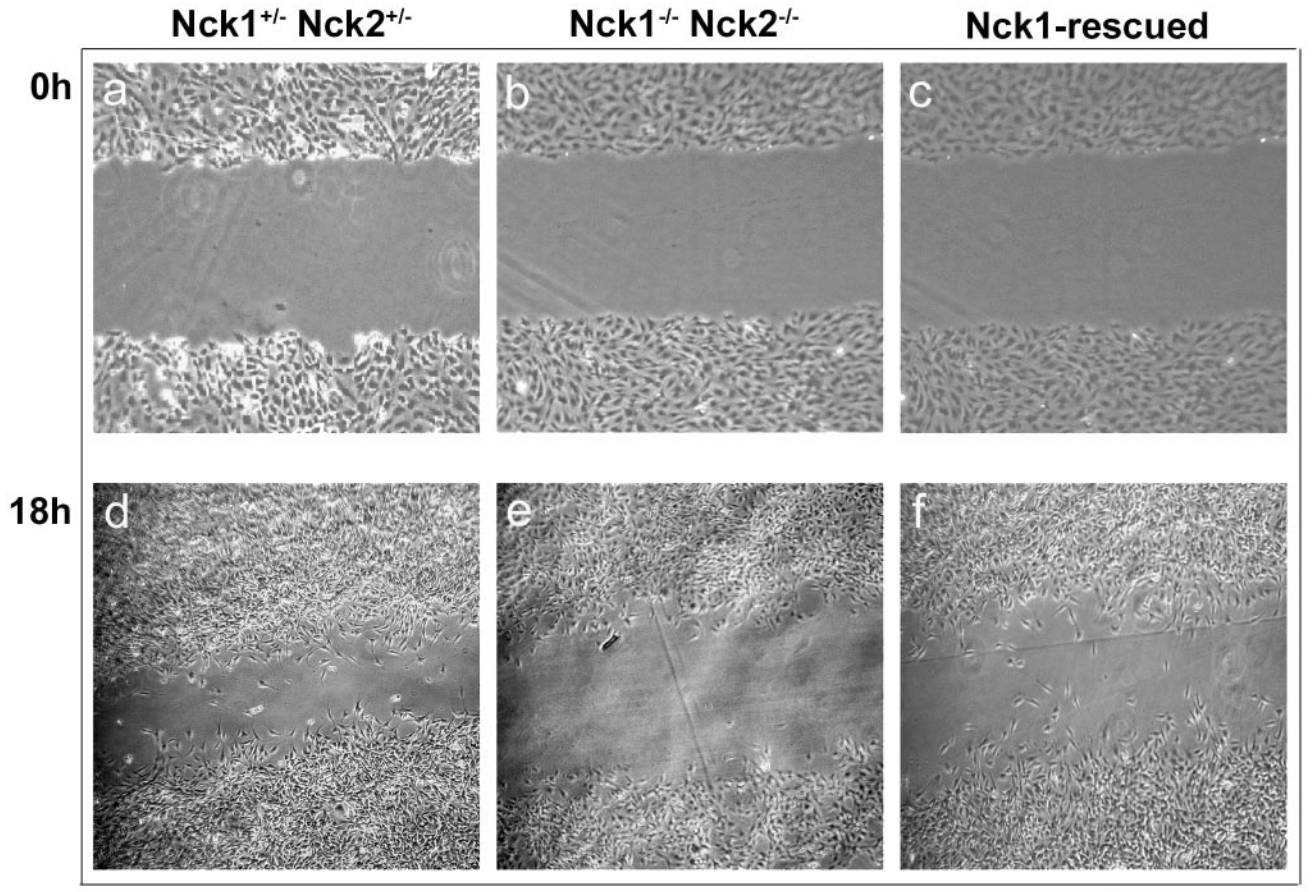

FIG. 7. Impaired motility of Nck1$^{-/-}$ Nck2$^{-/-}$ MEFs. Confluent monolayers of Nck1$^{+/-}$ Nck2$^{+/-}$, Nck1$^{-/-}$ Nck2$^{-/-}$, and Nck1-rescued MEFs were mechanically interrupted, and the inflicted wounds were photographed at the indicated time points (in hours). Nck1$^{-/-}$ Nck2$^{-/-}$ cells exhibited reduced ability to migrate into the wound compared to Nck1$^{+/-}$ Nck2$^{+/-}$ and Nck1-rescued MEFs.

embryos. Furthermore, the overlapping patterns of Nck1 and Nck2 expression may translate into mutually compensatory functional activities, at least during embryogenesis, and explain the apparently normal development of Nck1$^{-/-}$ and Nck2$^{-/-}$ single mutant mice.

Altered motility of embryonic fibroblasts derived from Nck1$^{-/-}$ Nck2$^{-/-}$ embryos. Our finding that the Nck proteins play a crucial role in the development of the notochord prompted us to further investigate this issue by generating MEF lines from Nck1$^{-/-}$ Nck2$^{-/-}$ embryos. We reasoned that the mesodermal defect apparent in Nck1$^{-/-}$ Nck2$^{-/-}$ embryos might be accounted for by abnormal migration or altered proliferative activity. To test the first hypothesis, the migratory activity of Nck1$^{-/-}$ Nck2$^{-/-}$ MEFs was compared by using an in vitro "wound" assay. To ensure that cell motility, rather than proliferation, would account for the presence of cells in the wounded area, MEF cultures were brought to quiescence by serum deprivation for a minimum of 24 h prior to inflicting the wound. Nck1$^{-/-}$ Nck2$^{-/-}$ MEFs (Fig. 7b and e) were unable to migrate and repopulate the wounded area at a rate comparable to Nck1$^{+/-}$ Nck2$^{+/-}$ MEFs (Fig. 7a and d). To rule out the possibility that this migratory defect was due to intrinsic clonal variations, Nck1$^{-/-}$ Nck2$^{-/-}$ MEFs were infected with retroviral vectors containing a bicistronic message encoding either the full-length human myc-tagged Nck1 cDNA and the fluorescent marker enhanced green fluorescent protein (EGFP; Nck1-IRES-EGFP) or IRES-EGFP alone and used as controls for the in vitro wound assay. The levels of expression of Nck1/EGFP in the infected Nck1$^{-/-}$ Nck2$^{-/-}$ MEFs were verified by flow cytometry and Western blot analysis (see Fig. 1C), and cells were divided by cell sorting into two subsets (Nck1/EGFP^{low} and Nck1/EGFP^{high} MEFs), according to the EGFP fluorescence intensity. Western blot analysis of Nck1/EGFP^{low} MEFs revealed Nck1 protein levels comparable to those of Nck1$^{+/-}$ Nck2$^{+/-}$ MEFs (Fig. 1C). In vitro, both Nck1/EGFP^{low} and Nck1/EGFP^{high} MEFs exhibited a migratory activity that was similar to that of Nck1$^{+/-}$ Nck2$^{+/-}$ MEFs and greater than that of Nck1$^{-/-}$ Nck2$^{-/-}$ MEFs (Fig. 7c and f). In contrast, we found no difference between the growth rates of either subset of Nck1/EGFP MEFs and Nck1$^{-/-}$ Nck2$^{-/-}$ MEFs, as assessed by the relative increase in cell number after a 48-h interval (data not shown). These results indicate that inactivation of the Nck proteins results in a significant impairment of fibroblast cell motility in vitro but has no obvious effect on proliferative activity.

Loss of Nck protein function results in altered lamellipodium formation. The apparent defect in motility of the mutant fibroblasts might reflect underlying abnormalities in cytoskel-

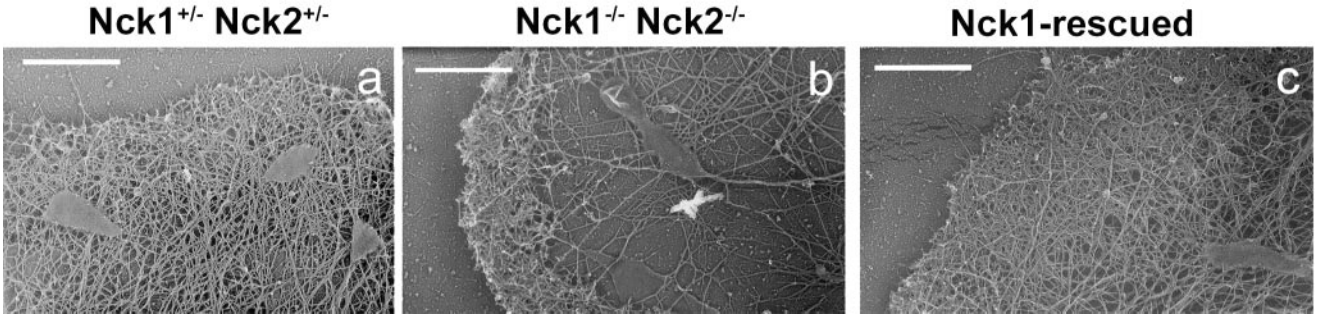

FIG. 8. Altered lamellipodium formation in Nck1$^{-/-}$ Nck2$^{-/-}$ MEFs. Platinum replica electron microscopy of lamellipodia of Nck1$^{-/-}$ Nck2$^{+/-}$, Nck1$^{-/-}$ Nck2$^{-/-}$, and Nck1-rescued MEFs, plated on fibronectin, was done. (a) In Nck1$^{+/-}$ Nck2$^{+/-}$ MEFs, a dense actin filament network of ca. 1 μm thick, the "leading edge," protruded out of a finely branched actin filamentous meshwork. (b) In Nck1$^{-/-}$ Nck2$^{-/-}$ MEFs, the leading edge was shorter and irregularly shaped and exhibited, at the ultrastructural level, short actin filaments. Furthermore, in the area immediately behind the leading edge, the actin filaments were consistently much sparser and less branched. (c) In the Nck1-rescued MEFs, the leading edge was characterized by an actin filament network of density comparable to that of Nck1$^{+/-}$ Nck2$^{+/-}$ MEFs. Scale bar, 1 μm.

etal architecture, and we therefore examined the actin filament network in Nck1$^{-/-}$ Nck2$^{-/-}$ MEFs by platinum replica electron microscopy and analyzed lamellipodial formation under basal conditions and during cytoskeletal recovery after ATP starvation. In these sets of experiments, we compared Nck1$^{-/-}$ Nck2$^{-/-}$ MEFs infected with IRES-EGFP retroviral vector (simply defined as Nck1$^{-/-}$ Nck2$^{-/-}$ MEFs) to the "Nck1-rescued" Nck1/EGFP^{high} MEFs and to Nck1$^{+/-}$ Nck2$^{+/-}$ MEFs. MEFs were plated on fibronectin-coated coverslips for 90 min and then fixed for electron microscopy. In Nck1$^{+/-}$ Nck2$^{+/-}$ MEFs, a dense actin filament network approximately 1-μm thick, corresponding to the cells' leading edge, protruded out of a finely branched actin filamentous meshwork (Fig. 8a). In Nck1$^{-/-}$ Nck2$^{-/-}$ MEFs, the leading edge was shorter, irregularly shaped, and exhibited short actin filaments at the ultrastructural level. Furthermore, in the area immediately behind the leading edge, the actin filaments were consistently much sparser and less branched (Fig. 8b). In the majority of Nck1-rescued MEFs, the leading edge was characterized by an actin filament network with a density comparable to that of Nck1$^{+/-}$ Nck2$^{+/-}$ MEFs (Fig. 8c). However, the phenotype of the Nck1-rescued MEFs exhibited some heterogeneity, with variations ranging between the two extremes depicted above, probably due to different Nck1 expression levels.

To investigate nascent lamellipodia under synchronous conditions, we examined cells recovering from ATP depletion (60). In the absence of glucose, sodium azide causes a rapid depletion of cellular ATP, which results in a reversible impairment of actin assembly, probably due to lack of bound actin monomers. Sodium azide washout is followed by a rapid restoration of actin assembly, which occurs as a synchronous burst of membrane protrusion. One minute after sodium azide washout, the recovery of Nck1$^{-/-}$ Nck2$^{-/-}$ MEFs was comparable or slightly faster than that of Nck1$^{+/-}$ Nck2$^{+/-}$ and Nck1-rescued MEFs (Fig. 9a and d). In contrast, after 20 min, the recovery of Nck1$^{-/-}$ Nck2$^{-/-}$ MEFs was significantly impaired compared to that of Nck1$^{+/-}$ Nck2$^{+/-}$ and Nck1-rescued MEFs (Fig. 9). Indeed, Nck1$^{-/-}$ Nck2$^{-/-}$ MEFs had shorter filaments at the leading edge and less-branched filaments behind the leading edge. Taken together, our findings indicate that the Nck proteins play a significant role in the formation of lamellipodia, a process driven by actin polymerization. These findings also suggest that the absence of functional Nck proteins does not inhibit the early stage of lamellipodial formation but probably affects the stability and extension of lamellipodia.

DISCUSSION

We used a genetic approach to address the expression and function of the mammalian Nck SH2/SH3 adaptors. To this end, we engineered mouse strains with mutations that place the β-galactosidase gene under the control of the Nck1 or Nck2 endogenous promoter and at the same time introduce deletions into the Nck1 or Nck2 coding sequence. Analysis of the resulting embryos indicates that the two Nck genes have a largely overlapping pattern of expression, are jointly required for embryonic development and, in particular, are important for placentation and axial rotation. Nck1$^{-/-}$ Nck2$^{-/-}$ embryos die in utero around gestational day 9.5 and exhibit, among other defects, severe alterations in mesoderm-derived structures, particularly in the organization of the notochord. Embryonic fibroblast lines derived from Nck1$^{-/-}$ Nck2$^{-/-}$ embryos have altered migratory properties and show defects in lamellipodium formation, revealing a significant physiological role for Nck in regulating the actin filament network, which may pertain to its in vivo functions.

With regard to expression, we have compared Nck1 and Nck2 in adult and embryonic tissues. For adult tissues, we analyzed protein extracts derived from either Nck1$^{-/-}$ or Nck2$^{-/-}$ mice. Unlike the more widely expressed Nck1, Nck2 was not detectable in the liver and in skeletal muscle and was present at low levels in brain extracts. This finding was confirmed by β-galactosidase staining of adult brain of heterozygous Nck1$^{IRES\text{-}lacZ}$ and Nck2$^{tau\text{-}lacZ}$, which showed a more restricted pattern of expression for Nck2 (data not shown). Both Nck1 and Nck2 were found at high levels in adult thymus and spleen, a finding consistent with observations implicating Nck in antigen-specific T-cell (63) and B-cell (39) receptor signaling. The potential role of Nck adaptors in the nervous and immune systems cannot currently be addressed because of the early lethality of Nck1$^{-/-}$ Nck2$^{-/-}$ embryos but is under investigation by conditional inactivation of the Nck genes.

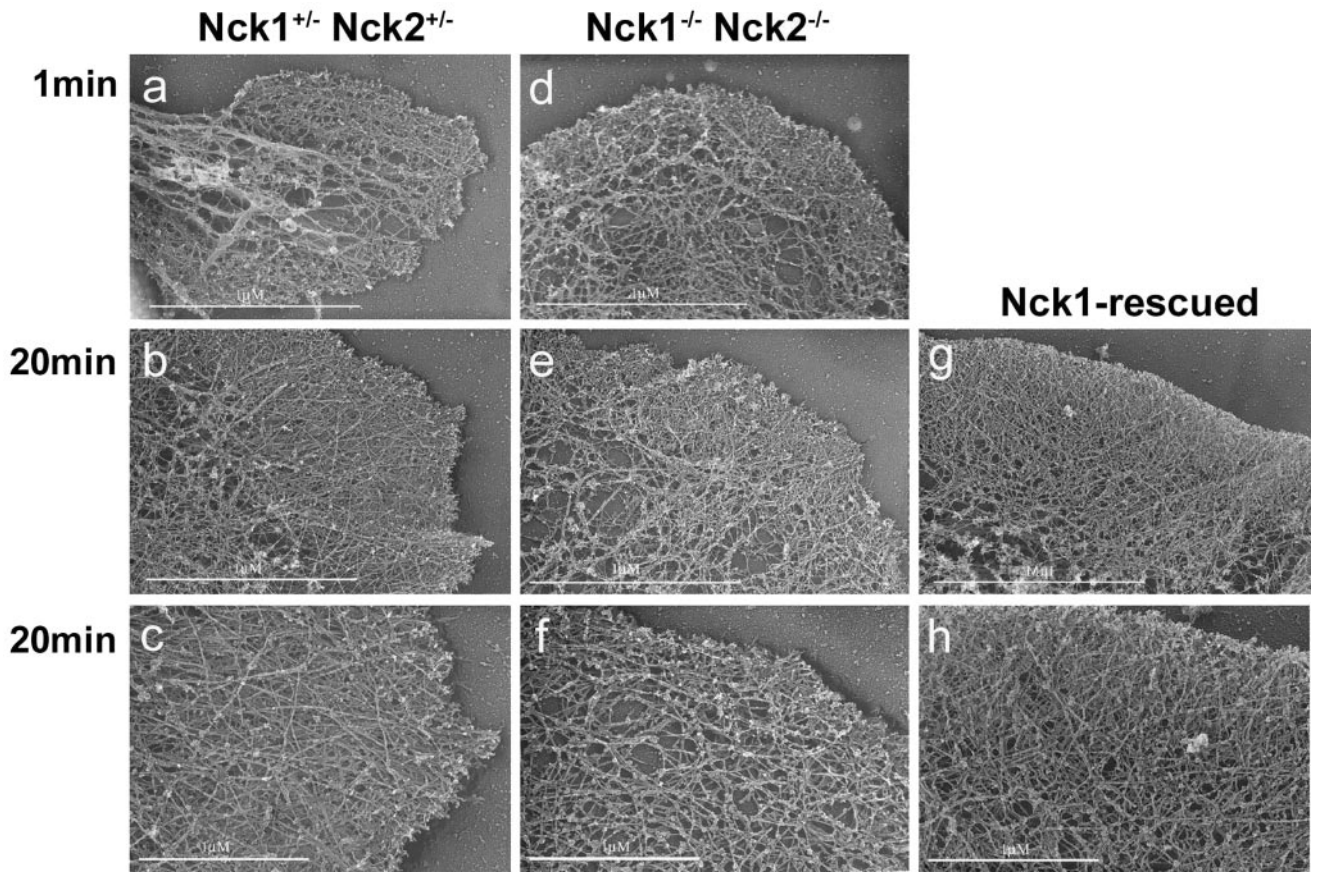

FIG. 9. Actin network organization upon ATP recovery. Platinum replica electron microscopy of lamellipodia of Nck1$^{+/-}$ Nck2$^{+/-}$, Nck1$^{-/-}$ Nck2$^{-/-}$, and Nck1-rescued MEFs after a 1- or 20-min recovery period from ATP depletion was completed. One minute after sodium azide washout, the recovery of Nck1$^{-/-}$ Nck2$^{-/-}$ MEFs was comparable to that of Nck1$^{+/-}$ Nck2$^{+/-}$ and Nck1-rescued MEFs. In contrast, after 20 min, the recovery of Nck1$^{-/-}$ Nck2$^{-/-}$ MEFs was significantly impaired compared to that of Nck1$^{+/-}$ Nck2$^{+/-}$ and Nck1-rescued MEFs. Nck1$^{-/-}$ Nck2$^{-/-}$ MEFs had shorter filaments at the leading edge and less-branched filaments behind the leading edge.

The expression of Nck1 and Nck2 during early embryonic development was investigated by β-galactosidase staining of mice heterozygous for the Nck$^{\text{IRES-lacZ}}$ or Nck2$^{\text{tau-lacZ}}$ alleles. At E7.5, both Nck genes were expressed in the allantois and headfold but, at later stages, Nck1 remained broadly expressed, whereas Nck2 appeared mainly restricted to developing nervous system, endoderm, and mesodermal derivatives, particularly the notochord and somites. Although inactivation of Nck1 or Nck2 was compatible with normal pre- and postnatal development, mutation of both Nck1 and Nck2 resulted in early embryonic lethality, indicating that the functions of Nck1 and Nck2 are overlapping, mutually compensatory, and essential for embryonic development.

Nck1$^{-/-}$ Nck2$^{-/-}$ embryos exhibited alterations in mesoderm-derived structures, such as notochord and somites, and neural ectoderm. These defects may be directly due to the loss of Nck function in these structures. Alternatively, the abnormal development of the notochord may be the primary defect, which causes secondary abnormalities in patterning of the neural tube and somatic derivatives (5, 12). Our finding that late but not early notochord development (two to four somites) was affected by loss of Nck function suggests that the Nck genes products may not be required for initial notochord formation but rather prevent notochord degeneration and/or promote anterior progression of mesodermal precursor cells from the primitive streak or node. This hypothesis is also supported by preliminary findings that Nck is expressed at the late-streak stage in the node (data not shown), the source of notochord progenitors (3, 28, 58). These observations warrant further investigation by chimeric analysis.

The mechanisms responsible for axial rotation in the embryo are not completely understood. Several lines of evidence suggest that the faster growth rate of the neural tube compared to the underlying endodermal structures (26) and notochord development (27) may be decisive factors. It is tempting to speculate that in Nck1$^{-/-}$ Nck2$^{-/-}$ embryos the fragmentation, midline displacement, and bifurcation of the notochord may disrupt the hard core around which the embryo normally revolves, thereby inhibiting the physiologic turning of the embryo. The phenotype of Nck1$^{-/-}$ Nck2$^{-/-}$ embryos is strikingly similar to that of Csk$^{-/-}$ mice (25, 40) and partially overlaps with that of fibronectin$^{-/-}$ (21), α5 integrin$^{-/-}$ (66), and focal adhesion kinase$^{-/-}$ (FAK) (18) mice but is distinct from that of Nik$^{-/-}$ embryos (65). Although embryos deficient for components of the fibronectin pathway lack somites and exhibit a more severe phenotype, Csk$^{-/-}$, fibronectin$^{-/-}$, α5 inte-

grin$^{-/-}$, FAK$^{-/-}$, and Nck1$^{-/-}$ Nck2$^{-/-}$ mutants share abnormalities in the notochord, axial rotation, and chorioallantoic fusion. In contrast, the mesodermal defect of Nik$^{-/-}$ embryos is targeted to the somites and spares the integrity of the notochord and processes such as chorioallantoic fusion and axial rotation. Furthermore, the defect of Nik$^{-/-}$ embryos is cell nonautonomous and results from defective migration of mesodermal precursor from the primitive streak. It is tempting to speculate that the binding of Nck to components of the integrin signaling pathway (for a review, see reference 7) may underlie the defects common to Nck1$^{-/-}$ Nck2$^{-/-}$, Csk$^{-/-}$, fibronectin$^{-/-}$, α5 integrin$^{-/-}$, and FAK$^{-/-}$ embryos by regulating the migratory properties of mesodermal precursors through cell adhesion.

To pursue the potential role of Nck in cell migration suggested by the mutant phenotype, we analyzed the actin filament network of fibroblast cell lines from Nck1$^{-/-}$ Nck2$^{-/-}$ E8.5 embryos by platinum replica electron microscopy. Cell migration has been proposed to require four steps: extension of actin-rich protrusions, such as lamellipodia, formation of new adhesions, cell body contraction, and tail detachment (32). Nck1$^{-/-}$ Nck2$^{-/-}$ MEFs exhibit defective migration and differ morphologically from Nck1-rescued controls under basal conditions and during recovery after ATP depletion. The reduced density, length, and disorganization of actin filaments at the leading edge and its adjacent region indicate that Nck plays a role in lamellipodial formation. The defective migration of Nck1$^{-/-}$ Nck2$^{-/-}$ fibroblasts was confirmed upon Cre-mediated deletion of Nck2 in Nck1$^{-/-}$ fibroblasts, further supporting the hypothesis that Nck genes are essential in cytoskeletal plasticity (unpublished results). Interactions of Nck with proteins such as Pak, N-WASP, and WAVE (4, 14, 37) may underlie this phenomenon. It will be of interest to analyze the contribution of each of these Nck-mediated pathways in physiologic cell movement. N-WASP mutant mice have been generated and display prominent neural tube and cardiac abnormalities and alterations in the actin-based motility of certain intracellular pathogens (53). However, the general formation of actin-containing structures appeared to be unaffected. The relatively mild phenotype of N-WASP-deficient cells in comparison to Nck-deficient fibroblasts is consistent with the view that Nck proteins also regulate other mediators of actin polymerization, such as WAVE.

In conclusion, our results shed light on the in vivo functions of mammalian Nck1 and Nck2 and reveal an essential role in embryogenesis. The involvement of Nck in actin reorganization and cell motility in culture provides a cellular basis for understanding the in vivo functions of these SH2/SH3 adaptors.

ACKNOWLEDGMENTS

We thank Louise Larose for the Nck1-specific antibody, Jill Meisenhelder for helpful discussion, and Jim Fawcett for critically reading the manuscript.

This work was supported by grants from the Canadian Institutes of Health Research (CIHR) and the National Cancer Institute of Canada. T.P. is a distinguished investigator of the CIHR.

REFERENCES

1. **Anton, I. M., W. Lu, B. J. Mayer, N. Ramesh, and R. S. Geha.** 1998. The Wiskott-Aldrich syndrome protein-interacting protein (WIP) binds to the adaptor protein Nck. J. Biol. Chem. **273:**20992–20995.
2. **Becker, E., U. Huynh-Do, S. Holland, T. Pawson, T. O. Daniel, and E. Y. Skolnik.** 2000. Nck-interacting Ste20 kinase couples Eph receptors to c-Jun N-terminal kinase and integrin activation. Mol. Cell. Biol. **20:**1537–1545.
3. **Beddington, R. S.** 1994. Induction of a second neural axis by the mouse node. Development **120:**613–620.
4. **Bokoch, G. M., Y. Wang, B. P. Bohl, M. A. Sells, L. A. Quilliam, and U. G. Knaus.** 1996. Interaction of the Nck adapter protein with p21-activated kinase (PAK1). J. Biol. Chem. **271:**25746–25749.
5. **Brand-Saberi, B., and B. Christ.** 2000. Evolution and development of distinct cell lineages derived from somites. Curr. Top. Dev. Biol. **48:**1–42.
6. **Braverman, L. E., and L. A. Quilliam.** 1999. Identification of Grb4/Nck β, an Src homology 2 and 3 domain-containing adapter protein having similar binding and biological properties to Nck. J. Biol. Chem. **274:**5542–5549.
7. **Buday, L., L. Wunderlich, and P. Tamas.** 2002. The Nck family of adapter proteins: regulators of actin cytoskeleton. Cell Signal **14:**723–731.
8. **Candia, A. F., J. Hu, J. Crosby, P. A. Lalley, D. Noden, J. H. Nadeau, and C. V. Wright.** 1992. Mox-1 and Mox-2 define a novel homeobox gene subfamily and are differentially expressed during early mesodermal patterning in mouse embryos. Development **116:**1123–1136.
9. **Chen, M., H. She, E. M. Davis, C. M. Spicer, L. Kim, R. Ren, M. M. Le Beau, and W. Li.** 1998. Identification of Nck family genes, chromosomal localization, expression, and signaling specificity. J. Biol. Chem. **273:**25171–25178.
10. **Chen, M., H. She, A. Kim, D. T. Woodley, and W. Li.** 2000. Nck β adapter regulates actin polymerization in NIH 3T3 fibroblasts in response to platelet-derived growth factor bb. Mol. Cell. Biol. **20:**7867–7880.
11. **Cowan, C. A., and M. Henkemeyer.** 2001. The SH2/SH3 adaptor Grb4 transduces B-ephrin reverse signals. Nature **413:**174–179.
12. **Dockter, J., and C. P. Ordahl.** 2000. Dorsoventral axis determination in the somite: a re-examination. Development **127:**2201–2206.
13. **Echelard, Y., D. J. Epstein, B. St. Jacques, L. Shen, J. Mohler, J. A. McMahon, and A. P. McMahon.** 1993. Sonic hedgehog, a member of a family of putative signaling molecules, is implicated in the regulation of CNS polarity. Cell **75:**1417–1430.
14. **Eden, S., R. Rohatgi, A. V. Podtelejnikov, M. Mann, and M. W. Kirschner.** 2002. Mechanism of regulation of WAVE1-induced actin nucleation by Rac1 and Nck. Nature **418:**790–793.
15. **Edwards, D. C., L. C. Sanders, G. M. Bokoch, and G. N. Gill.** 1999. Activation of LIM-kinase by Pak1 couples Rac/Cdc42 GTPase signalling to actin cytoskeletal dynamics. Nat. Cell Biol. **1:**253–259.
16. **Fawcett, J., and T. Pawson.** 2000. Signal transduction. N-WASP regulation: the sting in the tail. Science **290:**725–726.
17. **Frischknecht, F., V. Moreau, S. Rottger, S. Gonfloni, I. Reckmann, G. Superti-Furga, and M. Way.** 1999. Actin-based motility of vaccinia virus mimics receptor tyrosine kinase signalling. Nature **401:**926–929.
18. **Furuta, Y., D. Ilic, S. Kanazawa, N. Takeda, T. Yamamoto, and S. Aizawa.** 1995. Mesodermal defect in late phase of gastrulation by a targeted mutation of focal adhesion kinase, FAK. Oncogene **11:**1989–1995.
19. **Galisteo, M. L., J. Chernoff, Y. C. Su, E. Y. Skolnik, and J. Schlessinger.** 1996. The adaptor protein Nck links receptor tyrosine kinases with the serine-threonine kinase Pak1. J. Biol. Chem. **271:**20997–21000.
20. **Garrity, P. A., Y. Rao, I. Salecker, J. McGlade, T. Pawson, and S. L. Zipursky.** 1996. *Drosophila* photoreceptor axon guidance and targeting requires the dreadlocks SH2/SH3 adapter protein. Cell **85:**639–650.
21. **George, E. L., E. N. Georges-Labouesse, R. S. Patel-King, H. Rayburn, and R. O. Hynes.** 1993. Defects in mesoderm, neural tube and vascular development in mouse embryos lacking fibronectin. Development **119:**1079–1091.
22. **Gruenheid, S., R. DeVinney, F. Bladt, D. Goosney, S. Gelkop, G. D. Gish, T. Pawson, and B. B. Finlay.** 2001. Enteropathogenic *E. coli* Tir binds Nck to initiate actin pedestal formation in host cells. Nat. Cell Biol. **3:**856–859.
23. **Hing, H., J. Xiao, N. Harden, L. Lim, and S. L. Zipursky.** 1999. Pak functions downstream of Dock to regulate photoreceptor axon guidance in *Drosophila*. Cell **97:**853–863.
24. **Holland, S. J., N. W. Gale, G.D.Gish, R. A. Roth, Z. Songyang, L. C. Cantley, M. Henkemeyer, G. D. Yancopoulos, and T. Pawson.** 1997. Juxtamembrane tyrosine residues couple the Eph family receptor EphB2/Nuk to specific SH2 domain proteins in neuronal cells. EMBO J. **16:**3877–3888.
25. **Imamoto, A., and P. Soriano.** 1993. Disruption of the csk gene, encoding a negative regulator of Src family tyrosine kinases, leads to neural tube defects and embryonic lethality in mice. Cell **73:**1117–1124.
26. **Jacobson, A. G., and P. P. Tam.** 1982. Cephalic neurulation in the mouse embryo analyzed by SEM and morphometry. Anat. Rec. **203:**375–396.
27. **Keller, R., L. Davidson, A. Edlund, T. Elul, M. Ezin, D. Shook, and P. Skoglund.** 2000. Mechanisms of convergence and extension by cell intercalation. Philos. Trans. R. Soc. Lond. B Biol. Sci. **355:**897–922.
28. **Kinder, S. J., T. E. Tsang, M. Wakamiya, H. Sasaki, R. R. Behringer, A. Nagy, and P. P. Tam.** 2001. The organizer of the mouse gastrula is composed of a dynamic population of progenitor cells for the axial mesoderm. Development **128:**3623–3634.
29. **Kulkarni, S. V., G. Gish, P. van der Geer, M. Henkemeyer, and T. Pawson.** 2000. Role of p120 Ras-GAP in directed cell movement. J. Cell Biol. **149:**457–470.

30. **Kuriyan, J., and D. Cowburn.** 1997. Modular peptide recognition domains in eukaryotic signaling. Annu. Rev. Biophys. Biomol. Struct. **26:**259–288.
31. **Lai, K. M., and T. Pawson.** 2000. The ShcA phosphotyrosine docking protein sensitizes cardiovascular signaling in the mouse embryo. Genes Dev. **14:** 1132–1145.
32. **Lauffenburger, D. A., and A. F. Horwitz.** 1996. Cell migration: a physically integrated molecular process. Cell **84:**359–369.
33. **Lehmann, J. M., G. Riethmuller, and J. P. Johnson.** 1990. Nck, a melanoma cDNA encoding a cytoplasmic protein consisting of the src homology units SH2 and SH3. Nucleic Acids Res. **18:**1048.
34. **Li, N., A. Batzer, R. Daly, V. Yajnik, E. Skolnik, P. Chardin, D. Bar-Sagi, B. Margolis, and J. Schlessinger.** 1993. Guanine-nucleotide-releasing factor hSos1 binds to Grb2 and links receptor tyrosine kinases to Ras signalling. Nature **363:**85–88.
35. **Li, W., P. Hu, E. Y. Skolnik, A. Ullrich, and J. Schlessinger.** 1992. The SH2 and SH3 domain-containing Nck protein is oncogenic and a common target for phosphorylation by different surface receptors. Mol. Cell. Biol. **12:**5824–5833.
36. **Lock, L. S., I. Royal, I., M. A. Naujokas, and M. Park.** 2000. Identification of an atypical Grb2 carboxyl-terminal SH3 domain binding site in Gab docking proteins reveals Grb2-dependent and -independent recruitment of Gab1 to receptor tyrosine kinases. J. Biol. Chem. **275:**31536–31545.
37. **Lu, W., S. Katz, R. Gupta, and B. J. Mayer.** 1997. Activation of Pak by membrane localization mediated by an SH3 domain from the adaptor protein Nck. Curr. Biol. **7:**85–94.
38. **Margolis, B., O. Silvennoinen, F. Comoglio, C. Roonprapunt, E. Skolnik, A. Ullrich, and J. Schlessinger.** 1991. High-efficiency expression/cloning of epidermal growth factor-receptor-binding proteins with Src homology 2 domains. Proc. Natl. Acad. Sci. USA **89:**8894–8898.
39. **Mizuno, K., Y. Tagawa, K. Mitomo, N. Watanabe, T. Katagiri, M. Ogimoto, and H. Yakura.** 2002. Src homology region 2 domain-containing phosphatase 1 positively regulates B-cell receptor-induced apoptosis by modulating association of B-cell linker protein with Nck and activation of c-Jun NH2-terminal kinase. J. Immunol. **169:**778–786.
40. **Nada, S., T. Yagi, H. Takeda, T. Tokunaga, H. Nakagawa, Y. Ikawa, M. Okada, and S. Aizawa.** 1993. Constitutive activation of Src family kinases in mouse embryos that lack Csk. Cell **73:**1125–1135.
41. **Nishimura, R., W. Li, A. Kashishian, A. Mondino, M. Zhou, J. Cooper, and J. Schlessinger.** 1993. Two signaling molecules share a phosphotyrosine-containing binding site in the platelet-derived growth factor receptor. Mol. Cell. Biol. **13:**6889–6896.
42. **Obermeier, A., S. Ahmed, E. Manser, S. C. Yen, C. Hall, and L. Lim.** 1998. PAK promotes morphological changes by acting upstream of Rac. EMBO J. **17:**4328–4339.
43. **Park, D.** 1997. Cloning, sequencing, and overexpression of SH2/SH3 adaptor protein Nck from mouse thymus. Mol. Cells **7:**231–236.
44. **Park, D., and S. G. Rhee.** 1992. Phosphorylation of Nck in response to a variety of receptors, phorbol myristate acetate, and cyclic AMP. Mol. Cell. Biol. **12:**5816–5823.
45. **Pawson, T.** 1995. Protein modules and signalling networks. Nature **373:**573–580.
46. **Rivero-Lezcano, O. M., A. Marcilla, J. H. Sameshima, and K. C. Robbins.** 1995. Wiskott-Aldrich syndrome protein physically associates with Nck through Src homology 3 domains. Mol. Cell. Biol. **15:**5725–5731.
47. **Rohatgi, R., P. Nollau, H. Y. Ho, M. W. Kirschner, and B. J. Mayer.** 2001. Nck and phosphatidylinositol 4,5-bisphosphate synergistically activate actin polymerization through the N-WASP-Arp2/3 pathway. J. Biol. Chem. **276:** 26448–26452.
48. **Rozakis-Adcock, M., R. Fernley, J. Wade, T. Pawson, and D. Bowtell.** 1993. The SH2 and SH3 domains of mammalian Grb2 couple the EGF receptor to the Ras activator mSos1. Nature **363:**83–85.
49. **Ruan, W., P. Pang, and Y. Rao.** 1999. The SH2/SH3 adaptor protein dock interacts with the Ste20-like kinase misshapen in controlling growth cone motility. Neuron **24:**595–605.
50. **Sanders, L. C., F. Matsumura, G. M. Bokoch, and P. de Lanerolle.** 1999. Inhibition of myosin light chain kinase by p21-activated kinase. Science **283:**2083–2085.
51. **Saxton, T. M., B. G. Ciruna, D. Holmyard, S. Kulkarni, K. Harpal, J. Rossant, and T. Pawson.** 2000. The SH2 tyrosine phosphatase shp2 is required for mammalian limb development. Nat. Genet. **24:**420–423.
52. **Schlaepfer, D. D., M. A. Broome, and T. Hunter.** 1997. Fibronectin-stimulated signaling from a focal adhesion kinase-c-Src complex: involvement of the Grb2, p130cas, and Nck adaptor proteins. Mol. Cell. Biol. **17:**1702–1713.
53. **Snapper, S. B., F. Takeshima, I. Anton, C. H. Liu, S. M. Thomas, D. Nguyen, D. Dudley, H. Fraser, D. Purich, M. Lopez-Ilasaca, C. Klein, L. Davidson, R. Bronson, R. C. Mulligan, F. Southwick, R. Geha, M. B. Goldberg, F. S. Rosen, J. H. Hartwig, and F. W. Alt.** 2001. N-WASP deficiency reveals distinct pathways for cell surface projections and microbial actin-based motility. Nat. Cell Biol. **3:**897–904.
54. **Songyang, Z., S. E. Shoelson, M. Chaudhuri, G. Gish, T. Pawson, W. G. Haser, F. King, T. Roberts, S. Ratnofsky, R. J. Lechleider, et al.** 1993. SH2 domains recognize specific phosphopeptide sequences. Cell **72:**767–778.
55. **Stein, E., A. A. Lane, D. P. Cerretti, H. O. Schoecklmann, A. D. Schroff, R. L. Van Etten, and T. O. Daniel.** 1998. Eph receptors discriminate specific ligand oligomers to determine alternative signaling complexes, attachment, and assembly responses. Genes Dev. **12:**667–678.
56. **Su, Y. C., C. Maurel-Zaffran, J. E. Treisman, and E. Y. Skolnik.** 2000. The Ste20 kinase misshapen regulates both photoreceptor axon targeting and dorsal closure, acting downstream of distinct signals. Mol. Cell. Biol. **20:** 4736–4744.
57. **Suetsugu, S., H. Miki, and T. Takenawa.** 2002. Spatial and temporal regulation of actin polymerization for cytoskeleton formation through Arp2/3 complex and WASP/WAVE proteins. Cell Motil. Cytoskeleton **51:**113–122.
58. **Sulik, K., D. B. Dehart, T. Iangaki, J. L. Carson, T. Vrablic, K. Gesteland, and G. C. Schoenwolf.** 1994. Morphogenesis of the murine node and notochordal plate. Dev. Dyn. **201:**260–278.
59. **Svitkina, T. M., and G. G. Borisy.** 1998. Correlative light and electron microscopy of the cytoskeleton of cultured cells. Methods Enzymol. **298:**570–592.
60. **Svitkina, T. M., A. A. Neyfakh, Jr., and A. D. Bershadsky.** 1986. Actin cytoskeleton of spread fibroblasts appears to assemble at the cell edges. J. Cell Sci. **82:**235–248.
61. **Tanaka, M., W. Lu, R. Gupta, and B. J. Mayer.** 1997. Expression of mutated Nck SH2/SH3 adaptor respecifies mesodermal cell fate in *Xenopus laevis* development. Proc. Natl. Acad. Sci. USA **94:**4493–4498.
62. **Tu, Y., F. Li, and C. Wu.** 1998. Nck-2, a novel Src homology 2/3-containing adaptor protein that interacts with the LIM-only protein PINCH and components of growth factor receptor kinase-signaling pathways. Mol. Biol. Cell **9:**3367–3382.
63. **van Leeuwen, J. E., and L. E. Samelson.** 1999. T-cell antigen-receptor signal transduction. Curr. Opin. Immunol. **11:**242–248.
64. **Wilkinson, D. G., S. Bhatt, and B. G. Herrmann.** 1990. Expression pattern of the mouse T gene and its role in mesoderm formation. Nature **343:**657–659.
65. **Xue, Y., X. Wang, Z. Li, N. Gotoh, D. Chapman, and E. Y. Skolnik.** 2001. Mesodermal patterning defect in mice lacking the Ste20 NCK interacting kinase (NIK). Development **128:**1559–1572.
66. **Yang, J. T., H. Rayburn, and R. O. Hynes.** 1993. Embryonic mesodermal defects in alpha 5 integrin-deficient mice. Development **119:**1093–1105.